

# Flywheel-Type Tensile Impact Tester with a New Load Cell for Polymer Sheet and Film

MITSURU YOKOUCHI and YASUJI KOBAYASHI, *Department of Industrial Chemistry, Faculty of Technology, Tokyo Metropolitan University, Setagaya-ku Tokyo 158, Japan*

## Synopsis

A new load cell for flywheel-type impact tensile testing was designed and fabricated for specimens of polymer sheet and film. The cell employs a piezoelectric ceramic oscillator (toric in shape) as a load sensor, which has a high natural frequency (1800 kHz) and high sensitivity (ca. 0.1 V/N without amplification). The time constant for the electric circuit was improved substantially by the introduction of a voltage follower using an operational amplifier with excellent performance (common mode voltage  $\pm 120$  V and slew rate 100 V/ $\mu$ sec). The positioning of the load sensor and the shape of specimen clamps are important design features, especially the halved Morse-type taper pins in the structure of the specimen clamps. Signals of impact, passing through the piezoelectric oscillator and the voltage follower, are recorded by a transient time converter. The converter is equipped with a memorization system, an automatic pretrigger circuit, and a facility for reproduction under a slow time base, thus eliminating the need for troublesome photographing. For performance testing of the impact tester, oriented poly(ethylene terephthalate) sheets were used and good results were obtained.

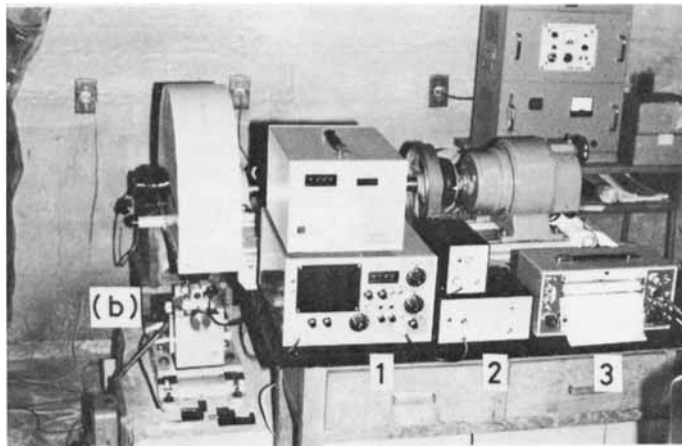
## INTRODUCTION

Thus far, various machines and methods have been developed for testing polymeric materials under impact loading where the experimental conditions are intended to simulate those encountered in practice.<sup>1</sup> Among them, a flywheel-type high-speed tensile tester<sup>2</sup> is considered to be a valid apparatus for polymer sheets and films from the following viewpoints. The impact strain speed can be changed over a wide range. The loss in flywheel velocity can be easily avoided if the inertia of the wheel is sufficient. It is easy to introduce and study the effect of various factors on the specimen (e.g., orientation and heat treatment). The testing results may be correlated directly with other physical properties (e.g., dynamic and/or dielectric relaxation measurements).

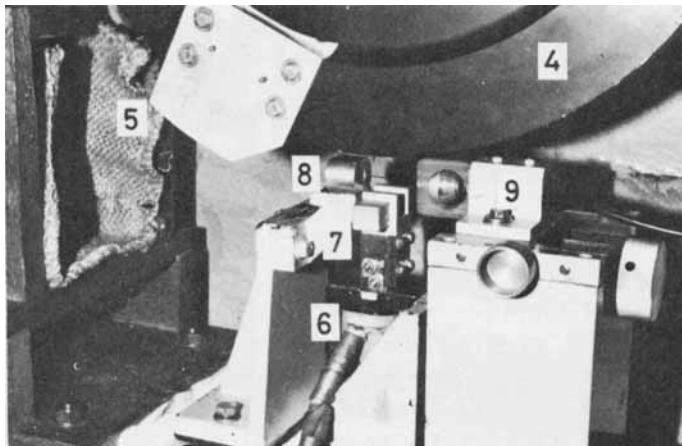
High-speed tensile testers designed thus far are limited by the performance of the conventional load cell, i.e., strain gauge force pickup. In the method where strain gauges are attached to an elastic metal, there is a tendency for the gauge to give an erroneous stress-time curve in the case of measurement of a relatively small tension applied to polymer sheets and films. The poor performance results because the natural frequency of metal and its sensitivity are reciprocal elements with respect to each other. In this study, the design and fabrication of a high-speed tensile impact tester with a new load cell is reported. Results of its performance using poly(ethylene terephthalate) sheets are presented. The load cell, based on a new principle, has a very high natural frequency and also a large output voltage, thus eliminating the need for an amplifier.

## APPARATUS

The apparatus described in this paper consists of the following four elements; (i) flywheel impacting assembly, (ii) load cell, (iii) specimen clamps, and (iv) recording device. A photograph of the high-speed tensile tester is shown in Figure 1 and the schematic diagram of the instrumentation is reproduced in Figure 2. To obtain meaningful and characteristic load-time curves, a few problems should be resolved: (a) utilizing a load sensing device with a fast response time and with low noise characteristics, (b) proper positioning of such a load cell, and (c) triggering of the sweep in recording.



(a)



(b)

Fig. 1. (a) General view of the flywheel-type impact tester and accessory instrumentation: (1) transient time converter, (2) voltage follower, and (3) balancing-type recorder. (b) Close-up of the main flywheel impacting arrangement: (4) flywheel, (5) striking fork, (6) solenoid, (7) struck block, (8) front clamp, and (9) load cell.

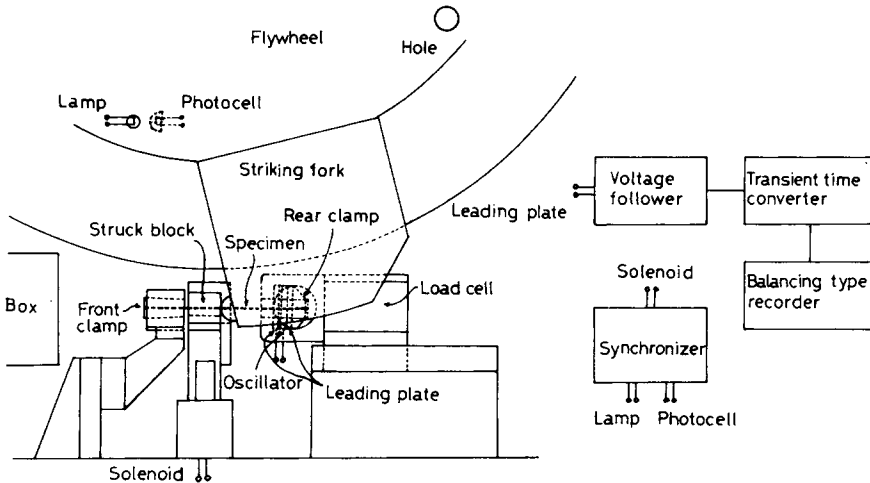


Fig. 2. Schematic diagram of the instrumentation.

### Flywheel Impacting Assembly

A steel flywheel 460 mm in diameter and 54 mm wide is rotated by a 400 W three-phase shunt motor at speeds from 50 to 1000 rpm. This range of speed was selected so that the inertia of the wheel is sufficient for the flywheel impacting assembly to bear the impact. Stress is applied through a struck block and a front clamp to the sample by means of a striking fork mounted on the rim of the flywheel. Since the distance between the center of the flywheel and the point of impact of the striking fork with the struck block is 251 mm, the impact tester can be operated at peripheral velocities from 1.3 to 26.3 m/sec.

The flywheel has a hole near the perimeter. The hole was designed so that the synchronizer functions as long as the light passes through it and is detected by the photocell. The position of the hole is at a point  $\frac{5}{6}$  of a revolution ahead of the point of contact of the striking fork and the struck block. After the flywheel has been adjusted to the operating speed, the synchronizer energizes a solenoid which forces up the struck block to the position of impact with the rotating striking fork. Then the struck block pushes the front clamp forward, which gives tension to the specimen (Fig. 2).

### Load Cell

The principle of conventional strain gauge force pickup is illustrated by adhering strain gauges to an elastic metal and converting the ohmic resistance change for metal elongation during application of a force to a voltage, followed by amplification. The introduction of this amplifier is liable to amplify various noises in the same instant and induce an erroneous sweep of recording as well as a deterioration in accuracy of the stress-time curve. On the other hand, the metal has an invariable natural frequency, which plays an important role in the noise in the stress-time curve. Owing to this noise, it is very difficult in impacting speeds from 1.3 to 26.3 m/sec to analyze the slope of the curve during the state of elastic deformation. The analysis is necessary to calculate the initial Young's modulus. Here we refer to the possibility of increasing the natural frequency of the metal. In general, the natural frequency ( $f$ ) of a rod can be related to the following equation:

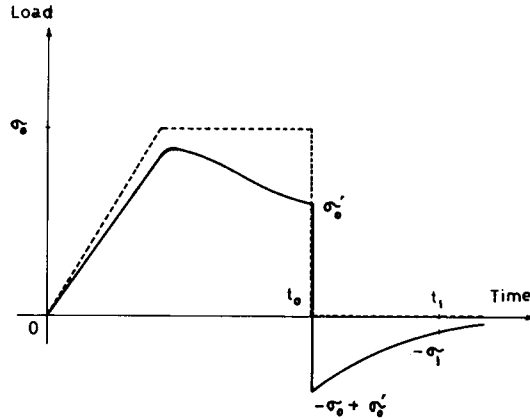


Fig. 3. Relationship between a real load- (broken line) and a recorded load- (solid line) time curve when the time constant of the electric circuit is  $\tau$ .

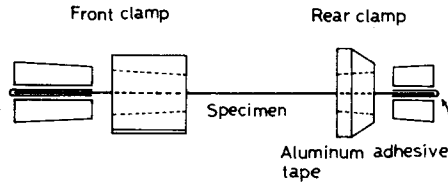


Fig. 4. Rear and front clamps for sheet and film specimens. The halved Morse-type taper pins are introduced through the centers of the clamps.

$$f \propto (\rho/l)^{1/2}$$

where  $\rho$  is density and  $l$  is length. For fast response, it is desirable for the metal to be of high density, but this may reduce the sensitivity. To increase the natural frequency also requires the length of the rod to be extensively short. In our experience, a solution to the above condition was not found.

Thereupon, a piezoelectric ceramic oscillator was adopted as a load sensor and a load cell was fabricated.<sup>3</sup> The following points were given particular attention in the design: (i) The length of the load cell was made as short as possible to restrain a rolling vibration. (ii) Considerations of weight and strength resulted in the choice of the fiber reinforced plastics (FRP) as the structural material of the load cell. FRP is also useful for insulation of the electric circuit containing the piezoelectric oscillator. (iii) The head part of the load cell was drilled along the tangential-line direction of the locus of the striking fork. The leading plates, oscillator, and rear clamp were placed there in order to convert the tensile force applied to the specimen directly to the compressive force through the rear clamp. Therefore, the shape of the piezoelectric oscillator and the leading plate is toric and the specimen passes through the center hole [Figs. 1(b) and 2]. (iv) Piercing in the transverse direction is required to facilitate the charging of the rear clamp with the specimen into the load cell.

The toric oscillator used here (Murata Seisakusho) has outer and inner diameters of 24 and 10 mm, respectively, and a thickness of 1 mm (natural frequency  $f = 1800$  kHz, dielectric constant  $\kappa' = 6400$  pF, internal resistance  $R_1 = 500$  M $\Omega$ , and voltage output ca. 0.1 V/N). Here we consider the time constant  $\tau$  of the electric circuit ( $= \kappa'R$ , where  $R$  is the input impedance). It is assumed

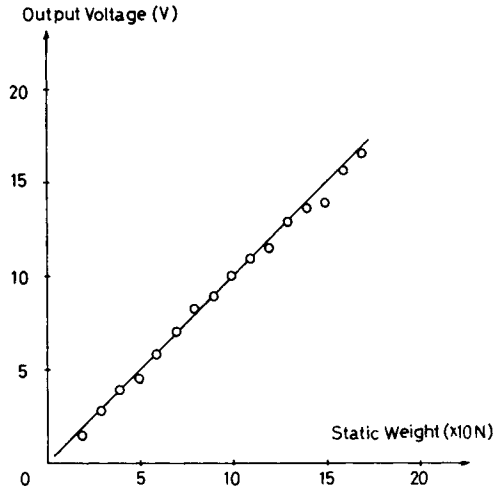


Fig. 5. Static calibration of load cell in tension.

that a load indicated by the broken line is really added; then, the recorded load-time curve becomes the one expressed in the solid owing to the electric relaxation determined by the time constant (Fig. 3). The relationship between them is formulated as follows:

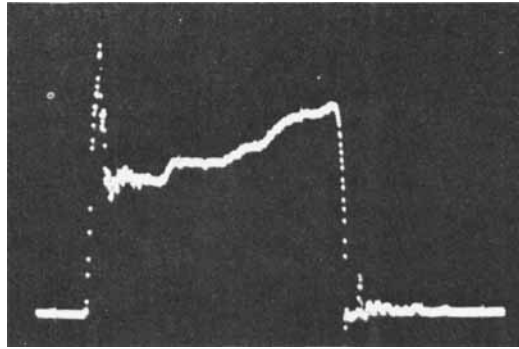
$$\sigma'_0 = \sigma_0 \exp(-t_0/\tau)$$

$$\tau = \Delta t / \ln[(\sigma_0 - \sigma'_0)/\sigma_1]$$

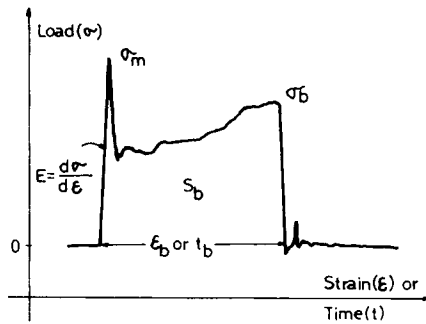
where  $\Delta t = t_1 - t_0$ . The symbols used in the above equations are defined in Figure 3. From the above relationship, it is clear that the longer  $\tau$  is, the less the difference. Since the recording device has an input impedance  $R_2 = 2 \text{ M}\Omega$ , the time constant was calculated as follows:  $\tau = \kappa' \cdot R_2 = 6400 \text{ pF} \cdot 2 \text{ M}\Omega = 12.8 \text{ msec}$ . The difference between the real and recorded load-time curves is remarkable in such a case where plastic deformation occurs, and the breaking time ranges over a few 10 msec. Therefore, we assembled a voltage follower and introduced it between the piezoelectric oscillator and the recording device. The operational amplifier (DATEL, input impedance  $R_3 = 10^{12} \Omega$ ) used features a high-voltage operation (common mode voltage:  $\pm 120 \text{ V}$ ) and a high-speed response (slew rate:  $100 \text{ V}/\mu\text{sec}$ ), and was incorporated in the form of all feedback. The apparent time constant was improved to the following value;  $\tau = \kappa' \cdot R_1 = 6400 \text{ pF} \cdot 500 \text{ M}\Omega = 3200 \text{ msec}$ . This made it possible to obtain meaningful and characteristic load-time curves for impact testing in the range of speeds from 1.3 to 26.3 m/sec.

### Specimen Clamps

There are two kinds of specimen clamps made of duralumin for mechanical strength and light weights: a rear clamp charged directly in the above load cell and a front clamp (Fig. 2). The characteristics of the rear clamp are as follows: (a) the clamp is within a structure which converts the tensile force through the leading plate to the compressive force uniformly along the whole surface of the toric oscillator, and (b) since halved Morse-type taper pins were introduced in the center of the clamp, the clamping of a specimen can be performed outside



(a)



(b)

Fig. 6. (a) Photograph of typical load-time impact curve of PET sheet with resolution of 25  $\mu$ sec on the cathode-ray tube of the transient time converter (400 rpm = 10.5 m/sec =  $1.8 \times 10^4$  %/sec at 20°C). (b) Recorded curve of (a) and the definition of five physical properties; initial Young's modulus  $E$ , maximum load  $\sigma_m$ , breaking load  $\sigma_b$ , breaking energy  $S_b$ , and breaking strain  $\epsilon_b$  (or breaking time  $t_b$ ).

the load cell and compression of the specimen is strong without accompanying slippage (Fig. 4). The front clamp was fabricated on the same principle. Considering the procedure for charging the specimen, there is a geometrical restriction in clamping with the front clamp. This was solved by making a special fixture.

### Recording Device

Signals passing through the piezoelectric oscillator and the voltage follower (not amplifying) are recorded by a transient time converter, TTC (Riken Denshi). This is suited to the handling of a fast single event, i.e., a transient waveform associated with impact, where the information can be stored in a semiconductor memory and reproduced under a slower time base at need, on a balancing-type recorder chart. Moreover, the self-contained cathode-ray tube always displays the memorized load-time curve. These eliminate the need for troublesome photographing. The curve is recorded (per one word within 5  $\mu$ sec at maximum resolution) to high-precision binary decimal bit digit code in the range of ca. 5 msec to 26 sec. This instrument is equipped also with an automatic pretrigger automatic memory circuit. Hence, there is no need for other mechanical or electric triggering systems and erroneous sweeps of recording were not found.

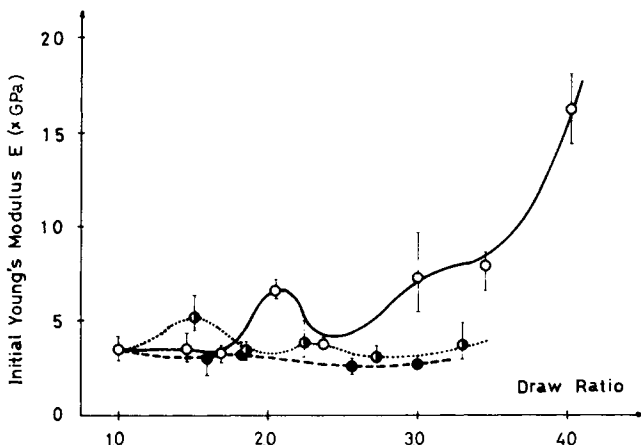


Fig. 7. Dependency of initial Young's modulus  $E$  on draw ratio and cutout angle ( $0^\circ$ , solid line,  $\circ$ ;  $30^\circ$ , dotted line,  $\circ$ ; and  $90^\circ$ , dashed line,  $\bullet$ ) to the elongated direction for PET sheet (400 rpm = 10.5 m/sec =  $1.8 \times 10^4$  %/sec at  $20^\circ\text{C}$ ).

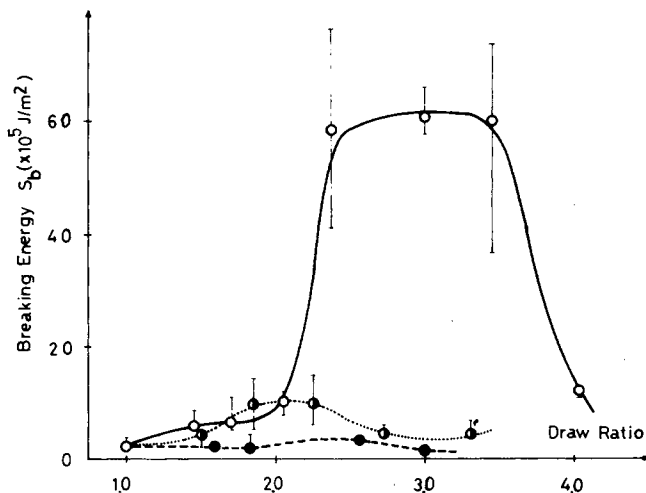


Fig. 8. Dependency of breaking energy  $S_b$  on draw ratio and cutout angle ( $0^\circ$ , solid line,  $\circ$ ;  $30^\circ$ , dotted line,  $\circ$ ; and  $90^\circ$ , dashed line,  $\bullet$ ) to the elongated direction for PET sheet (400 rpm = 1.5 m/sec =  $1.8 \times 10^4$  %/sec at  $20^\circ\text{C}$ ).

Figure 5 is a typical dead weight static calibration curve for the load cell. The output voltage was found to be ca. 0.1 V/N.

## PERFORMANCE TESTING

As a sample for performance testing of the fabricated impact tester, poly-(ethylene terephthalate) [PET [ $-\text{OCH}_2\text{CH}_2\text{O}-\text{CO}\phi\text{CO}-$ ] $_n$  sheet (Teijin, 260  $\mu\text{m}$  thickness and density 1.344) was used. This was uniaxially elongated at various times at  $80^\circ\text{C}$  in air (density 1.366 at draw ratio 4.2). Test specimens were prepared from the elongated sheet, having the dimensions  $5 \times 90$  mm. The cutout direction was varied from parallel to perpendicular to the elongated direction. Both end parts of the specimens were reinforced by adhesive tape made

of aluminum, the lengths of which corresponded with those of the rear and front halved Morse-type taper pins (Fig. 4).

Mechanical anisotropy occurs by uniaxial orientation. Since an accurate stress-time curve is observed in a very short time (several msec), the effect of relaxation of macromolecules is not significant and the microstructure of the test specimen (e.g., state of orientation) is reflected in the physical properties during impact tension. Figure 6(a) is a photograph of a typical memorized load-time impact curve of PET sheet on the cathode-ray tube of TTC and Figure 6(b) shows the recorded curve. Five physical properties are evident [Fig. 6(b)], i.e., initial Young's modulus  $E$ , maximum load  $\sigma_m$ , breaking load  $\sigma_b$ , breaking energy  $S_b$ , and breaking strain  $\epsilon_b$  (or breaking time  $t_b$ ). Some results of impact testing are shown for initial Young's modulus and breaking energy in Figures 7 and 8, respectively. It was found that the change of physical properties is not monotonous within  $30^\circ$  against the elongated direction and the behavior of orientation varies especially at draw ratios of about 1.5, 2.0, and 3.5. These results indicate good performance of the apparatus and give information regarding structure changes due to elongation.

## CONCLUSION

A high-speed impact tester with a new load cell has been developed for polymer sheet and film and provides accurate noise-free load-time curves. The apparatus is relatively simple to operate and can be used in routine laboratory testing. The instrument correlates the characteristics of impact tension with molecular motion and microstructure of polymeric substances.

The authors would like to express their thanks to Nikkei Densoku Co., Hitachi Ltd., and DATEL in Japan for their valuable advices, and to the machining shop of their university for help in manufacturing the apparatus. The financial support of the Ministry of Education through Scientific Grant No. 275477 is gratefully acknowledged.

## References

1. G. D. Patterson, Jr. and W. R. Smith, *J. Appl. Polym. Sci.*, **6**, 278 (1962).
2. G. D. Patterson, Jr. and W. H. Miller, *J. Appl. Polym. Sci.*, **4**, 291 (1960).
3. P. P. Kelly and T. J. Dunn, *Mater. Res. Stand.*, **3**, 545 (1963).

Received June 1, 1978

Revised July 13, 1978